ELSEVIER

Physica D 163 (2002) 191–216

PHYSICA D

www.elsevier.com/locate/physd

Synchrony, stability, and firing patterns in pulse-coupled oscillators

Pranay Goel, Bard Ermentrout*

Department of Mathematics, University of Pittsburgh, Pittsburgh, PA 15260, USA

Received 6 July 2001; received in revised form 15 October 2001; accepted 15 October 2001
Communicated by J.P. Keener

Abstract

We study non-trivial firing patterns in small assemblies of pulse-coupled oscillatory maps. We find conditions for the existence of waves in rings of coupled maps that are coupled bi-directionally. We also find conditions for stable synchrony in general all-to-all coupled oscillators. Surprisingly, we find that for maps that are derived from physiological data, the stability of synchrony depends on the number of oscillators. We describe rotating waves in two-dimensional lattices of maps and reduce their existence to a reduced system of algebraic equations which are solved numerically. © 2002 Published by Elsevier Science B.V.

Keywords: Pulse-coupled oscillators; Firing patterns; Synchrony; Neural models

1. Introduction

There have been many recent investigations of the behavior of coupled networks of neural oscillators. A large body of experimental data indicates that brief periods of oscillatory activity may be required for certain cognitive functions (see [12] for references). Many theoretical approaches have been applied to the general question of synchrony and phase-locking [3,19,29]. These include restriction of the models to simple neurons like integrate-and-fire [2,20,27], weak coupling [8,15,18], and simple topologies [5,6]. In many of these papers, the coupling is pulse-like lasting only briefly relative to the length of the cycle. In this paper, we focus on the behavior of such pulse-coupled oscillators motivated by the fact that the coupling between neurons is often through rapidly decaying synapses.

When a stable oscillator is briefly perturbed by a sufficiently small stimulus, then, the phase of the oscillator is shifted by an amount that depends on the timing of the perturbation [17,29]. The change in phase of the oscillator is called the phase-response curve (PRC). PRCs are popular among experimentalists as they provide a way to quantify the behavior of the system without knowing the underlying mechanisms responsible for the behavior. Indeed, PRCs have been computed for many biological oscillators [4,29] including neurons [23–26]. Stoop et al. [26] have used experimental PRCs to devise coupled map lattices for arrays of nearest neighbor coupled neurons. Canavier and

* Corresponding author. Tel.: +1-412-624-8324; fax: +1-412-624-8397.
E-mail address: bard@math.pitt.edu (B. Ermentrout).

PII: S0167-2789(01)00374-8

colleagues have taken a different approach and analyzed rings of uni-directionally coupled PRCs without forcing. Our approach is similar but not restricted to uni-directional coupling.

We first define PRCs and then derive a set of discontinuous differential equations representing the phases of the respective oscillators. We then derive a map which describes the timing difference for a single periodically forced PRC and for a pair of coupled PRCs. We generalize this to a map for N globally coupled oscillators and prove a stability result. Surprisingly, the stability depends on the number of oscillators. We then turn to a ring of nearest neighbor coupled PRCs and derive conditions for the existence of traveling waves as well as their stability. We numerically simulate the ring and a line of coupled PRCs to show the differences. Finally, we consider two-dimensional arrays of nearest neighbor coupled PRCs and show the existence of (apparently numerically stable) rotating waves.

2. Phase-response curves and coupled phase models

2.1. Defining the PRC

Suppose that a system has a stable limit cycle solution and that we are only interested in a particular event within that system. For example, we might only be interested in the times at which a given neuron fires an action potential. At some fixed time after a spike, we briefly perturb the system (e.g., we inject a current pulse into the neuron). This perturbation changes the time of the next spike. The change in timing is the PRC and it is a function of the magnitude and the timing of the perturbation. Let T be the natural period of the oscillation and let $t = 0, T, 2T, \dots$ be the times of successive events. Suppose that at $t = t_s \in [0, T)$, we perturb the trajectory. Then, the new firing time is $\hat{T}(t_s)$. A major assumption of PRC theory is that the events that occur after $t = \hat{T}(t_s)$ are at $t = \hat{T}(t_s) + T, \hat{T}(t_s) + 2T, \dots$. This says that the effect of the perturbation is only carried for one cycle; there is no memory of the perturbation once the event has occurred. This is a rather severe restriction, but, in practice, it often holds. (However, in [23], there is a small change in the next spike time due to the presence of a slow potassium current. That is, the second spike after the stimulus occurs at $t < \hat{T}(t_s) + T$, but this difference is quite small compared to the initial phase-shift due to the perturbation.) We define the PRC to be

$$\Delta(\phi) \equiv 1 - \frac{\hat{T}(T\phi)}{T}, \tag{1}$$

where $\phi \equiv t_s/T \in [0, 1)$ is the phase. Thus, $\Delta(\phi)$ is positive (negative) if the effect of the stimulus is to advance (retard) the time of the next event. Most neurons have PRCs that satisfy

$$\Delta(0) = \lim_{\phi \to 1^-} \Delta(\phi) = 0.$$

This means that the spike time is unchanged if the perturbation arrives at the onset of the spike. The PRCs computed for excitatory pyramidal neurons as well as inhibitory cortical neurons have this property. (An example of PRC from [23] is shown in Fig. 3; Fig. 1 in [26] shows PRCs for both excitatory and inhibitory perturbations.)

2.2. Some exactly computable PRCs

In this section, we briefly describe PRCs for several classical model oscillators which have appeared in the literature. The first example is the well-known integrate-and-fire model:

$$\frac{\mathrm{d}V}{\mathrm{d}t} = -V + I$$

with $V(t^+) = 0$ when $V(t^-) = 1$. We assume that $I > 1$ so that this oscillates with a period of

$$T = -\ln \frac{I-1}{I}.$$

At $t = t_s$, we add an amount a to V and then ask when the oscillator will fire next. If the t_s is close enough to $t = T$ then the perturbation a will lift V past 1 and the oscillator will fire immediately so that $\hat{T}(t_s) = t_s$. Otherwise, an elementary calculation shows that

$$\hat{T}(t_s) = -\ln \frac{I-1}{I - a\,\mathrm{e}^{t_s}}.$$

Fig. 1a shows the PRC for the integrate-and-fire model for $I = 1.05$ and various values of a. For $a > 0$, the PRC never satisfies $\Delta(0) = 0$ and for $a < 0$ it satisfies neither the condition that $\Delta(0) = 0$ nor $\Delta(1) = 0$.

Another version of the integrate-and-fire model is the "quadratic" integrate-and-fire equation:

$$\frac{\mathrm{d}x}{\mathrm{d}t} = I + x^2$$

with firing defined at $x(t) \to \infty$ after which x is reset to $-\infty$. The period is just

$$T = \int_{-\infty}^{\infty} \frac{\mathrm{d}x}{I + x^2} = \frac{\pi}{\sqrt{I}}.$$

This model arises as the normal form for a limit cycle near a saddle-node (see [9,16]). As above, we assume that at $t = t_s$ a perturbation of size a is given. Then, an elementary calculation (see, e.g. [16]) shows that

$$\hat{T}(t_s) = t_s + \frac{1}{\sqrt{I}}\left(\frac{\pi}{2} - \arctan\left[\frac{a}{\sqrt{I}} - \cot(\sqrt{I}t_s)\right]\right).$$

In Fig. 1b, we show the PRC for $I = 1$ and various values of a. Unlike the integrate-and-fire model, the PRC for this model vanishes at both 0 and T regardless of the strength of the perturbation. In this sense, it is a much "better" representation of what a real neuron does.

As a final example, we take the classic radial isochron clock [11, p. 107], a two-dimensional system that is a simplified normal form for any system near a Hopf bifurcation:

$$\frac{\mathrm{d}r}{\mathrm{d}t} = \Lambda r(1 - r^2), \qquad \frac{\mathrm{d}\theta}{\mathrm{d}t} = 1.$$

This is the polar form of the oscillator, so $\theta \in S^1$. Firing is defined as $\theta = 0$ and perturbations are defined as shifts in the x-coordinate of length a. The parameter Λ is assumed to be very large so that perturbations are immediately brought back to the limit cycle along radii (see Fig. 2). In order for "phase" to be defined, we require that $|a| < 1$. As above, t_s is the time after firing that the pulse is given so that in the plane, $(x, y) = (\cos t_s, \sin t_s)$. After the pulse, the coordinates are $(a + \cos t_s, \sin t_s)$. The new angle, θ is obtained from trigonometry:

$$\tan\theta = \frac{\sin t_s}{a + \cos t_s},$$

thus

$$\hat{T}(t_s) = t_s + 2\pi - \arctan\left(\frac{\sin t_s}{a + \cos t_s}\right).$$

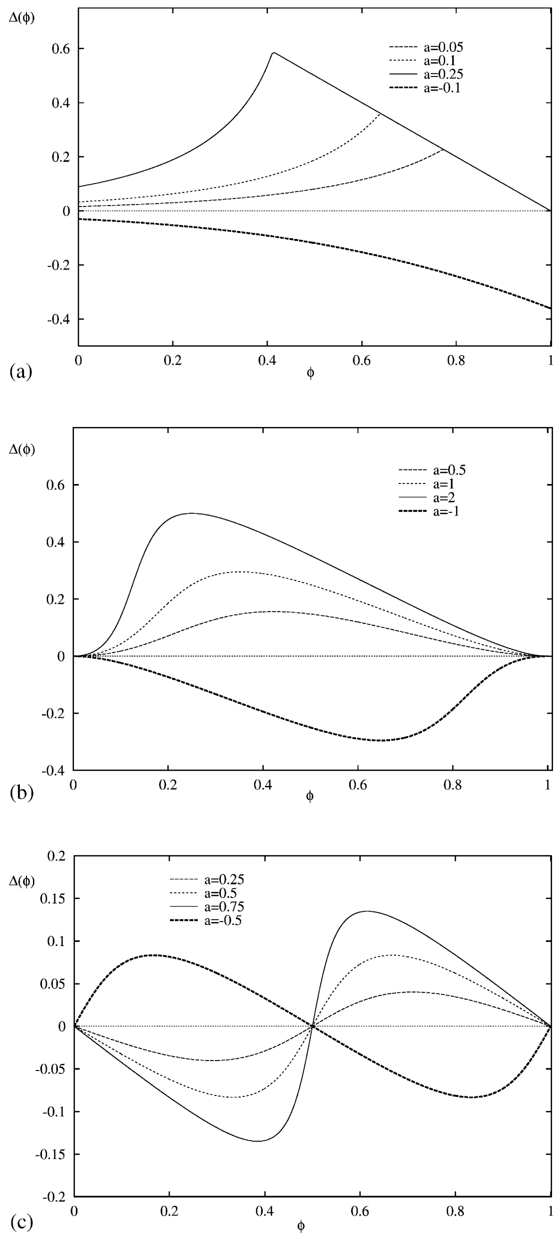

Fig. 1. The PRCs for the integrate-and-fire model (a); the quadratic integrate-and-fire model (b) and the radial isochron clock (c).

Fig. 1c shows the PRC for the radial isochron clock. Unlike the other two models, for a given value of a, the PRC can both advance and delay the firing. As $a \to 1$ the PRC becomes singular. Note that no matter what the value of a the PRC vanishes at $t = 0, T$. For small values of a, the radial isochron clock PRC has a particularly simple form

$$\Delta(\phi) = -\frac{a}{2\pi} \sin 2\pi\phi. \tag{2}$$

We will use this form later on when we analyze coupling in lattices.

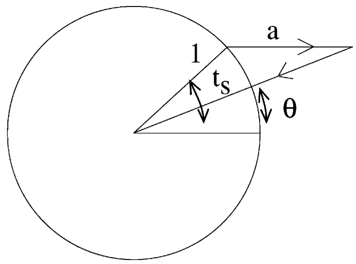

Fig. 2. The effect of a perturbation on the radial isochron clock.

Cortical neuron PRCs that have been measured generally either strictly advance (for positive perturbations) or delay (for negative perturbations) the phase. However, other neural PRCs can both advance and delay. (See, e.g. the PRCs computed for the firefly, *Pteroptyx malaccae* [4, Fig. 4], and the fruitfly *Drosophila pseudoobscura* pupae [29, Figs. 5–7, p. 414]. These PRCs looks similar to the small a version of the radial isochron clock.) It is easy to compute the PRC for model neurons as well. Mato et al. do this for the Hodgkin–Huxley model and the Connor–Stevens model. In the former, the PRC both advances and delays while in the latter, the PRC only advances the phase. In cortical PRCs such as measured by Reyes and Fetz [23,24], we find the following two classes of functions to be a good fit:

$$\Delta_1(\phi) = a\frac{\phi(1-\phi)}{1+\mathrm{e}^{-c(\phi-b)}} \tag{3}$$

with $c \geq 0$, $0 < b < 1$ and

$$\Delta_2(\phi) = a\phi(1-\phi)\,\mathrm{e}^{-p\phi-q(1-\phi)} \tag{4}$$

with $0 < p < q$. These are plotted in Fig. 3 along with the data from Reyes and Fetz [23]. Parameters for the fits were chosen using least squares. The former function provides a better fit, however, the latter allows us more flexibility in varying the shape of the PRC.

2.3. Coupling with PRCs

Suppose that one has computed a PRC. Then how can we use this to analyze the coupling between oscillators. The easiest way to think about this is to first consider a single oscillator that is periodically driven with a pulsatile stimulus. Assume that every P time units, a stimulus of strength a is given to the system. Then the phase right *before* the time of the nth stimulus is

$$\hat{\theta}_n = \theta_{n-1} + \frac{P}{T},$$

where θ_{n-1} is the phase right *after* the $(n-1)$th stimulus. The phase after the nth stimulus is thus

$$\theta_n = \hat{\theta}_n + \Delta(\hat{\theta}_n) = \theta_{n-1} + \frac{P}{T} + \Delta\left(\theta_{n-1} + \frac{P}{T}\right),$$

which gives a map for the phase. Let $\phi = \theta + P/T$. Then we get the more standard map:

$$\phi_n = \frac{P}{T} + \phi_{n-1} + \Delta(\phi_{n-1}) \equiv \frac{P}{T} + F(\phi_{n-1}). \tag{5}$$

We call $F(\phi) = \phi + \Delta(\phi)$ the *phase transition map* and it describes what the new phase is as a function of the old phase. This class of circle maps has been analyzed by many people. Glass and Mackey [11] provide a good overview of circle maps. We note here that if $F'(\phi) > 0$ then the map is invertible and there is no chaotic behavior.

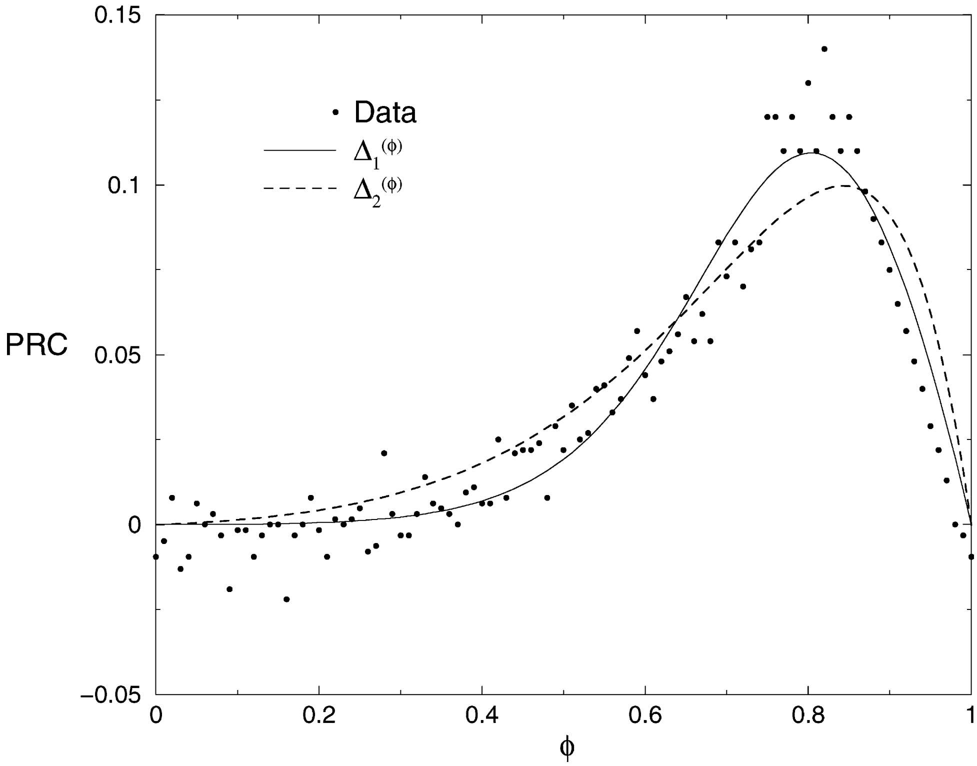

Fig. 3. Experimentally measured PRC [23] and two approximations.

Another way to formally describe the periodic driving is to embed the map into a discontinuous differential equation:

$$\frac{d\theta}{dt} = \frac{1}{T} + \delta_P(t)\Delta(\theta),$$

where

$$\delta_P(t) = \sum_n \delta(t - nP),$$

and $\delta(t)$ is the Dirac-delta function. The solution to this differential equation between the nth and $(n+1)$th stimulus is just

$$\theta(t) = \theta(nP) + \Delta(\theta(nP)) + \frac{t}{T},$$

and if we let ϕ_n be as defined as the phase right after the nth stimulus, $\phi_n = \theta(nP) + \Delta[\theta(nP)]$, then we get the map (5). This formal version of the forced map leads us easily to the obvious way of coupling PRCs:

$$\frac{d\theta_j}{dt} = \frac{1}{T_j} + C \sum_{n,k} \delta(t - t_k^n)\Delta_{jk}(\theta_j), \tag{6}$$

where t_k^n is the nth time that the kth oscillator fires, $\Delta_{jk}(\theta)$ the effect on the phase of the jth oscillator by the kth oscillator firing, and C the overall coupling strength. Note that $\Delta_{jk} = 0$ if oscillator k is not connected to oscillator j.

Dror et al. and Canavier et al. assume this form of coupling in their series of papers. Hoppensteadt and Izhikevich derive a similar model from synaptically coupled neurons near a saddle-node bifurcation. Winfree [28] replaces the Dirac-delta functions with a smooth pulsatile periodic function. The case of all-to-all coupling of the Winfree model was recently analyzed by Ariaratnam and Strogatz [1]. Ermentrout and Kopell [10] also replace the delta functions with smooth functions and analyze the resulting systems of equation. They derive the smoothed version from general neural net equations.

Stoop et al. [26] consider an alternative means of coupling between PRCs which is akin to "diffusive" coupling and coupled map lattices:

$$\phi_j(n+1) = (1-C)F(\phi_j(n)) + \frac{C}{m}\sum_k F(\phi_k(n)),$$

where the sum is over connections and m the number of such connections. A biological interpretation of this form of coupling was not suggested.

2.4. "Weak" coupling

Before turning to our results on "strong" coupling, we consider a limiting case when C is small. We assume that $1/T_j = 1 + \epsilon\omega_j$, where $C = \epsilon \ll 1$ is a small number. We let $\theta_j(t) = t + \phi_j(t)$. For ϵ small, $t_j^n \approx n + \phi_j(t)$ so we obtain

$$\frac{\mathrm{d}\phi_j}{\mathrm{d}t} = \epsilon\left(\omega_j + \sum_{k,n}\delta(t-n+\phi_k)\Delta_{jk}(t+\phi_j)\right).$$

Averaging this over one period leads to

$$\frac{\mathrm{d}\phi_j}{\mathrm{d}t} = \epsilon\left(\omega_j + \sum_{k}\Delta_{jk}(\phi_j-\phi_k)\right) + \mathrm{O}(\epsilon^2). \tag{7}$$

Phase equations such as this have been analyzed by numerous authors and have been shown to have many different non-trivial phase-locked solutions [8]. Thus, it should not be surprising that (6) also has a variety of different complex behaviors. We note that a phase-locked solution to (7) has the form

$$\phi_j = \Omega t + \bar{\psi}_j,$$

where $\bar{\psi}_j$ is a constant and Ω a constant determined from the equations. A sufficient (but not necessary) condition for stability of this solution is $\Delta'_{jk}(\bar{\psi}_j - \bar{\psi}_k) \le 0$.

2.5. Smooth pulsatile coupling

One other way to approach the instantaneous pulsatile coupling implicit in the definition of the PRC is to study a "smoothed" version:

$$\frac{\mathrm{d}\theta_j}{\mathrm{d}t} = \omega_j + \sum_k P(\theta_k)\Delta_{jk}(\theta_k),$$

where $P(\theta)$ is a smooth periodic pulse-like function centered at 0. For example,

$$P(\theta) = A_m(1+\cos\theta)^m,$$

where A_m is chosen so that the integral of P is 1. As m gets large, P will approach the Dirac-delta function. Winfree [28] first posed this class of models and recently Ariaratnam and Strogatz [1] analyzed the "all-to-all" coupled case for $m = 1$ and $\Delta_{jk}(\theta) = c\sin\theta$. In this brief section, we give a condition for the existence and stability of synchronous solutions. We assume the following:

(i) $\Delta_{jk}(\phi) = c_{jk}\Delta(\phi)$.

(ii) $c_{jk} = c_{kj}, \omega_j = \omega$,

$$\sum_k c_{jk} = c,$$

and the matrix, c_{ij} is irreducible.

(iii) There is a solution to

$$\phi' = \omega + cP(\phi)\Delta(\phi) \tag{8}$$

satisfying $\phi(t+T) = \phi(t) + 2\pi$ for some finite positive T.

The first assumption says that the responses to any perturbation differ only in magnitude. The second assumption says that the coupling is homogeneous, the oscillators are identical, the coupling is symmetric, and non-degenerate. The third assumption says the oscillators do not get stuck at fixed points. With these assumptions, a synchronous solution to

$$\frac{\mathrm{d}\theta_j}{\mathrm{d}t} = \omega + \sum_k c_{jk}P(\theta_k)\Delta(\theta_j) \tag{9}$$

exists, $\theta_j(t) = \phi(t)$. This is easily seen by substitution into (9) and using the homogeneity assumption and assumption (iii).

Suppose in addition, we have the following:

(iv) $c_{jk} \geq 0$.

(v) $Q \equiv \int_0^T P(\phi(t))\Delta'(\phi(t))\,\mathrm{d}t < 0$.

Then, the synchronous solution is asymptotically stable.

Remark. The integral Q is the generalization of the "XZ" loop conditions that Winfree derives for all-to-all coupling for pulse-coupled oscillators [28].

To prove this, we linearize (9): $\theta_j(t) = \phi(t) + y_j$. To the lowest order

$$\frac{\mathrm{d}y_j}{\mathrm{d}t} = \sum_k c_{jk}(P'(\phi(t))\Delta(\phi(t))y_j + P(\phi(t))\Delta'(\phi(t))y_j).$$

Recall that ϕ satisfies (8) so that if we differentiate this with respect to t we obtain:

$$\frac{\mathrm{d}\phi'(t)}{\mathrm{d}t} = (P'(\phi(t))\Delta(\phi(t)) + P(\phi(t))\Delta'(\phi(t)))\phi'(t).$$

Since $\phi'(t)$ is periodic, this means

$$\int_0^T P'(\phi(t))\Delta(\phi(t)) + P(\phi(t))\Delta'(\phi(t))\,\mathrm{d}t = 0$$

or

$$-\int_0^T P'(\phi(t))\Delta(\phi(t))\,\mathrm{d}t = \int_0^T P(\phi(t))\Delta'(\phi(t))\,\mathrm{d}t \equiv Q. \tag{10}$$

Let $\vec{\xi}$ be an eigenvector of the matrix c_{jk} with eigenvalue λ. Since c_{jk} is non-negative, irreducible, and symmetric, it has a unique eigenvector with non-negative components. (This is a consequence of the Frobenius–Perron theorem.) Since c_{jk} is homogeneous (i.e., its column sums are the same), this eigenvector is the vector of all 1's and the eigenvalue is c. Furthermore, since c_{jk} is non-negative and irreducible, this is the maximal eigenvalue. Thus, $c > \lambda$ for all $\vec{\xi} \neq \vec{1}$. The solutions to the linearized equation are

$$y_j(t) = x(t)[\vec{\xi}]_j,$$

where $x(t)$ is a scalar satisfying:

$$x'(t) = (cP(\phi(t))\Delta'(\phi(t)) + \lambda P'(\phi(t))\Delta(\phi(t)))x(t).$$

Integrating this over a period, we see that $x(t)$ will decay if and only if

$$M \equiv \int_0^T (cP(\phi(t))\Delta'(\phi(t)) + \lambda P'(\phi(t))\Delta(\phi(t)))\,\mathrm{d}t < 0.$$

Using (10), we see that

$$M = Q(c - \lambda).$$

Since $c > \lambda$, then a necessary and sufficient condition for stability of the synchronous state is that $Q < 0$ which is assumption (v). Note that there is a single zero eigenvalue corresponding to the time-translation invariance of the periodic solution.

We remark that this integral condition can be understood intuitively. Suppose that $\Delta'(\phi)$ is negative near the origin. (For example, in the radial isochron clock, this is true.) Suppose that $P(\phi)$ is positive and rapidly falls off to zero away from the origin. Then the integral quantity, Q will be negative as required. We also remark that this condition is analogous to the condition for the weakly coupled case. Indeed, the "weak interaction" function is

$$H(\phi) = \frac{1}{T}\int_0^T \Delta(t+\phi)P(t)\,\mathrm{d}t.$$

The condition for stability of the synchronous state is $H'(0) < 0$ which is equivalent to $Q < 0$.

3. Two oscillators

We now consider a pair of mutually coupled PRCs and derive a one-dimensional map. For simplicity we will assume identical frequencies. We assume that the function $F(x) = x + \Delta(x)$ is invertible ($F'(x) > 0$). This has several important consequences:

1. No stimulus can cause a neuron to fire immediately. The phase can be advanced but never sufficiently to induce instant firing. This means that if $x < 1$ then $F(x) < 1$ as well. Since $F(1) = 1$ and F is monotone increasing $F(x) < 1$ for $x < 1$.
2. Similarly, invertibility means that the phase of an oscillator can never be brought below 0.

This assumption holds if the coupling is not too strong.

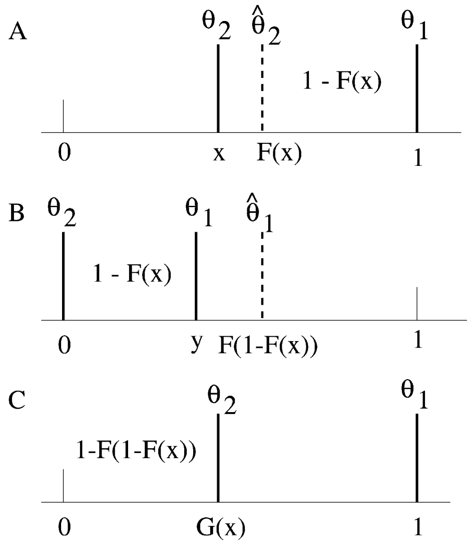

Fig. 4. Construction of the map, $x \mapsto G(x)$ for a pair of coupled PRCs.

3.1. Locking

We assume identical frequencies in order to obtain an ordering principle for the oscillators. The pair of oscillators satisfies the formal differential equation:

$$\frac{\mathrm{d}\theta_1}{\mathrm{d}t} = 1 + \sum_k \delta(t - t_2^k)\Delta(\theta_1), \qquad \frac{\mathrm{d}\theta_2}{\mathrm{d}t} = 1 + \sum_k \delta(t - t_1^k)\Delta(\theta_2),$$

where $t_{1,2}^k$ are the times at which oscillators 1 and 2 fire. Suppose that θ_1 is ahead of θ_2, then invertibility of F implies that θ_1 will always be ahead of θ_2 if they have identical frequencies. This is because the firing of θ_1 can never push θ_2 past 1 nor can θ_2 pull θ_1 below 0. If the frequencies are different, then it becomes more difficult to describe a map. Fig. 4 describes the construction of the map. Suppose that at the moment that θ_1 crosses 1, $\theta_2 = x$. Then immediately after firing, the new phase of θ_2 is $\hat{\theta}_2 = F(x)$. θ_1 is reset to 0 and θ_2 will then fire at $t = 1 - F(x)$ by which time θ_1 has advanced to $y = 1 - F(x)$. θ_1 is mapped to $\hat{\theta}_1 = F(y) = F(1 - F(x))$. It takes $1 - F(1 - F(x))$ amount of time for θ_1 to again reach 1 completing the map. Thus, the new value of θ_2 is found to be

$$x \to 1 - F(1 - F(x)) = x + \Delta(x) - \Delta(1 - x - \Delta(x)) \equiv G(x). \tag{11}$$

Fixed points of this map satisfy

$$0 = \Delta(x) - \Delta(1 - x - \Delta(x)).$$

If $\Delta(0) = 0$ as we usually assume, then $x = 0$ is always a fixed point. That is, there is a synchronous solution. There can be other fixed points as well; generically at least one interior fixed point. For the maps (2)–(4) there are two roots: the synchronous root and the anti-synchronous root. The maps arising from both the radial isochron clock and the integrate-and-fire model also have two fixed points: a synchronous and anti-synchronous root. The quadratic integrate-and-fire map is degenerate, $G(x) = x$.

An alternate way of deriving a map is to consider the timing rather than the phases of the oscillators. Let T_1 be the last time that oscillator 1 fired and $T_2 > T_1$ be the last time that oscillator 2 fired. Let T_j' denote the next firing time of each oscillator. Then

$$T_1' = 1 + T_1 - \Delta(T_2 - T_1), \qquad T_2' = 1 + T_2 - \Delta(T_1' - T_2)$$

defines the firing time map since both oscillators have a frequency of 1. Letting $\phi = T_2 - T_1$ we recover the phase map.

3.2. Stability of the fixed points of the map

Let $\bar{x}$ be a fixed point of (11). Stability is found by linearizing about $\bar{x}$ leading to

$$G'(\bar{x}) = [1 + \Delta'(\bar{x})][1 + \Delta'(1 - \bar{x} - \Delta(\bar{x}))].$$

This is just the product of the derivative of the phase transition map evaluated at the phase of oscillator 1 when 2 fires and vice versa. Since each term is positive from the invertibility of $F(x)$, this means that the fixed point will be stable if the product of the terms is less than 1. In particular, the condition for stability of the synchronous solution is

$$\sigma = [1 + \Delta'(0^+)][1 + \Delta'(1^-)] < 1. \tag{12}$$

Note that it is important that we take the correct limits for the PRC as often, a PRC does not have a continuous derivative. We can visually look at the PRC and determine if synchrony will be stable. For example, in the simple map (2) if $a > 0$ then $\Delta'(0) = \Delta'(1) = -a$ and thus $\sigma = (1-a)^2 < 1$ provided that a is less than 2. For the maps illustrated in Fig. 3, $\Delta'(0^+) = a_0 > 0$ and $\Delta'(1^-) = -a_1 < 0$ so that $\sigma = 1 + a_0 - a_1 - a_0 a_1$. If a_j is not too large, then a sufficient condition for stability is that $a_1 > a_0$ which clearly holds in the maps of Fig. 3. Thus, synchrony is stable.

The antiphase solution is unstable for the maps illustrated in Fig. 3. For the simple sinusoidal map (2), we see that $\phi = \frac{1}{2}$ is the anti-phase root and that it is unstable for $a > 0$ and stable for $-2 < a < 0$. The synchronous state is stable and the anti-phase solution unstable for the radial isochron clock if $a > 0$ while for $a < 0$ the situation is reversed.

3.3. All-to-all coupling

While the majority of this paper is devoted to patterns seen with local coupling, we can say a few general things about the all-to-all coupled case in which every cell is identically connected to every other cell. This is reminiscent of the case studied by Mirollo and Strogatz [20] for pulse-coupled integrate-and-fire models. They show that all initial conditions outside a set of measure zero converge to the synchronized state. In order to study all-to-all coupling, we need to make an important preliminary observation. Suppose (as we have throughout the paper) that F is monotone and thus invertible. Then $1 \geq F(\theta_1) \geq F(\theta_2) \geq 0$ for all $1 \geq \theta_1 \geq \theta_2 \geq 0$. Thus, if oscillator 1 is ahead of oscillator 2, then after both receive stimuli, oscillator 1 is still ahead of oscillator 2. Furthermore, neither oscillator can be brought to firing by the stimulation nor can either oscillator be pushed to 0 since $F(1) = 1$ and $F(0) = 0$. This means that if we have an array of N all-to-all identically coupled oscillators, then the order of their firing is always preserved. To study the stability of synchrony, we will create a locally defined map after the perturbation away from synchrony is given. This perturbation will determine a set of firing times *which will be preserved*. We can now assume that they are labeled in the order of their firing and from this derive the $(N-1)$-dimensional map. The map is done in N pieces corresponding to the single firing of each of the N oscillators in a cycle. We will go through the case of $N = 3$ oscillators to illustrate how the map is constructed for general N. We label the oscillators $\theta_1, \theta_2, \theta_3$ and suppose that the firing order is 1–2–3. We start $\theta_1 = 1$ and $1 > \theta_2 > \theta_3 > 0$ and follow the evolution as θ_2, θ_3 fire and then θ_1 is brought up to firing. We define two variables x_2, x_3 which will represent the two oscillators *which are not firing* so that initially x_2 represents θ_2 and x_3 represents θ_3. However, when oscillator 2 fires, x_2 will represent oscillator 3 and x_3 will represent oscillator 1 which will now be the furthest back in phase since it fired most recently. Once oscillator 2 fires, x_2 becomes oscillator 1 and x_3 becomes oscillator 2 as oscillator 3 is the next in line to fire. Once oscillator 3 fires, it goes to the back of the line and waits for oscillator 1 to fire again. We define three maps:

$$M_\mathrm{a}(x_2, x_3) = (F(x_2), F(x_3)), \qquad M_\mathrm{b}(x_2, x_3) = (1 - x_2 + x_3, 1 - x_2),$$

and

$$M_\mathrm{c}(x_2, x_3) = (F(1 - x_2 + x_3), F(1 - x_2)) = M_\mathrm{a}(M_\mathrm{b}(x_2, x_3)).$$

The first map is the initial response of 2 and 3 to 1 firing. The time elapsing until 2 fires is thus $1 - x_2'$, where $x_2' = F(x_2)$. At this point oscillator 3 has advanced to $1 - x_2' + x_3'$ where $x_3' = F(x_3)$. This advance without a firing is map M_b. Now, right after oscillator 2 fires, oscillator 3 has a phase $F(1 - x_2' + x_3')$ and oscillator 1 has a phase $F(1 - x_2')$. This explains the form of M_c. We apply M_c one more time accounting for oscillator 3 firing. Finally, we apply M_b one more time to bring θ_1 up to the threshold for firing. Thus, the map is

$$(\theta_2, \theta_3) \to M_\mathrm{b} M_\mathrm{c} M_\mathrm{c} M_\mathrm{a}(\theta_2, \theta_3).$$

This is defined only in the domain

$$1 \geq \theta_2 \geq \theta_3 \geq 0,$$

which as we have already noted is an invariant under these maps. The generalization to $N > 3$ oscillators is immediate. Synchrony is a solution to this system. Stability is determined by linearizing about the fixed point, $(0, 0, \ldots, 0)$. We consider two cases. In the simplest case, we suppose that the PRC is continuously differentiable at the origin. That is, $\Delta'(0^+) = \Delta'(1^-)$. This is true for the radial isochron clock and for the PRC of the Hodgkin–Huxley equations. However, it appears not to be true for the PRCs of cortical neurons and the models (3) and (4). If the PRC is continuously differentiable then $F'(0) = F'(1) \equiv \alpha$. However, if the PRC is not continuously differentiable, then $F'(0) \equiv \alpha_0 \neq \alpha_1 \equiv F'(1)$. We will discuss this more difficult case shortly. In the former case, the linearized map is just

$$B = E^N \alpha^N,$$

where the general form of E (the linearization of M_b) is

$$E = \begin{pmatrix} -1 & 1 & 0 & 0 & \cdots & 0 \\ -1 & 0 & 1 & 0 & \cdots & 0 \\ \vdots & & & & & \\ -1 & 0 & 0 & \cdots & 0 & 1 \\ -1 & 0 & 0 & \cdots & 0 & 0 \end{pmatrix}.$$

The $(N - 1) \times (N - 1)$ matrix E is just a permuted transpose of a companion matrix so that its characteristic polynomial is

$$p_E(\lambda) = \lambda^{N-1} + \lambda^{N-2} + \cdots + \lambda + 1,$$

whose roots are just the Nth roots of unity different from 1. These sit exactly on the unit circle so that the roots of B have magnitude α^N. From this, we conclude that the synchronous fixed point is asymptotically stable if and only if $\alpha = F'(0) < 1$. "Excitatory coupling" for the Hodgkin–Huxley equations as well as for the radial isochron clock leads to locally stable synchrony with all-to-all coupling.

What about stability in the second case? Here, we no longer have the simple structure for the linearization. To see why, consider the synchronous solution $(0, \dots, 0)$. One can see that

$$M_{\mathrm{a}}(0, \dots, 0) = (1, \dots, 1)$$

so that linearization of $M_{\mathrm{b}} M_{\mathrm{a}}$ leads to the matrix:

$$A_1 = \mathrm{diag}(\alpha_1, \dots, \alpha_1) E.$$

However, application of M_{c} to the vector of 1's leads to

$$M_{\mathrm{c}}(1, \dots, 1) = (1, \dots, 1, 0),$$

and the linearization is

$$A_2 = \mathrm{diag}(\alpha_1, \dots, \alpha_1, \alpha_0) E.$$

Since $\alpha_0 \neq \alpha_1$ the matrix A_2 is not a scalar multiple of E. We continue in this manner up the chain of maps and find that at each point, we replace the bottom most α_1 by an α_0. We thus must study the spectrum of a matrix consisting of products of E and products of diagonal matrices which are not scalar multiples of the identity matrix. For example, for the case $N = 3$ the linearization is

$$B = \begin{pmatrix} -1 & 1 \\ -1 & 0 \end{pmatrix} \begin{pmatrix} -\alpha_1 & \alpha_1 \\ -\alpha_0 & 0 \end{pmatrix} \begin{pmatrix} -\alpha_1\alpha_0 & \alpha_1\alpha_0 \\ -\alpha_1\alpha_0 & 0 \end{pmatrix}.$$

For the cases $N = 3, 4$, the resulting matrices B are upper triangular and the eigenvalues can be explicitly read off of the diagonals. In the case of $N = 3$, the eigenvalues are $\alpha_0^2\alpha_1, \alpha_0\alpha_1^2$ while for $N = 4$ they are $\alpha_0^3\alpha_1, \alpha_0^2\alpha_1^2, \alpha_0\alpha_1^3$. We show that is a general form for the eigenvalues. Thus, synchrony will be linearly stable if and only if each of the terms $\alpha^k\alpha^\ell$ is less than 1. That is, we have the following theorem.

Theorem. *The $N - 1$ eigenvalues of B are of the form*: $\alpha_0^\ell \alpha_1^{N-\ell}$, *where* $1 \le \ell < N$. *Synchrony is stable for an N-dimensional all-to-all coupled PRC network if each of these is less than* 1.

The proof of this theorem is given in Appendix A.

This has an interesting implication. Suppose that $\alpha_0 > 1$ and $\alpha_1 < 1$ as is the case for the experimentally computed PRCs. Suppose that $\alpha_0\alpha_1 < 1$ so that a pair stably synchronizes. Since $\alpha_0 > 1$, we can find a sufficiently large k such that $\alpha_0^k\alpha_1 > 1$ so that a network with $k + 1$ cells coupled in an all-to-all fashion does not have a stable synchronous solution while any smaller network does have a stable synchronous solution. The critical network size is thus $N = k + 1$, where k is the smallest integer larger than

$$-\frac{\log \alpha_1}{\log \alpha_0}.$$

For the cortical PRCs, α_0 is very close to 1 so that the network would have to be very large. However, it is easy to construct a simple PRC for which synchrony is stable for a pair but not for a three oscillator system. Take $\Delta(\theta) = a|\sin \pi\theta|/\pi$. Then $\alpha_0 = 1 + a$ and $\alpha_1 = 1 - a$. Synchrony is stable for the pair since the eigenvalue is $\alpha_0\alpha_1 = 1 - a^2$. However, for a network of three oscillators, the maximum eigenvalue is $\alpha_0^2\alpha_1 = 1 + a - a^2 - a^3$ which is greater than 1 if $a < \frac{1}{2}(\sqrt{5} - 1) \approx 0.618$. Thus for small values of a synchrony is not a stable solution.

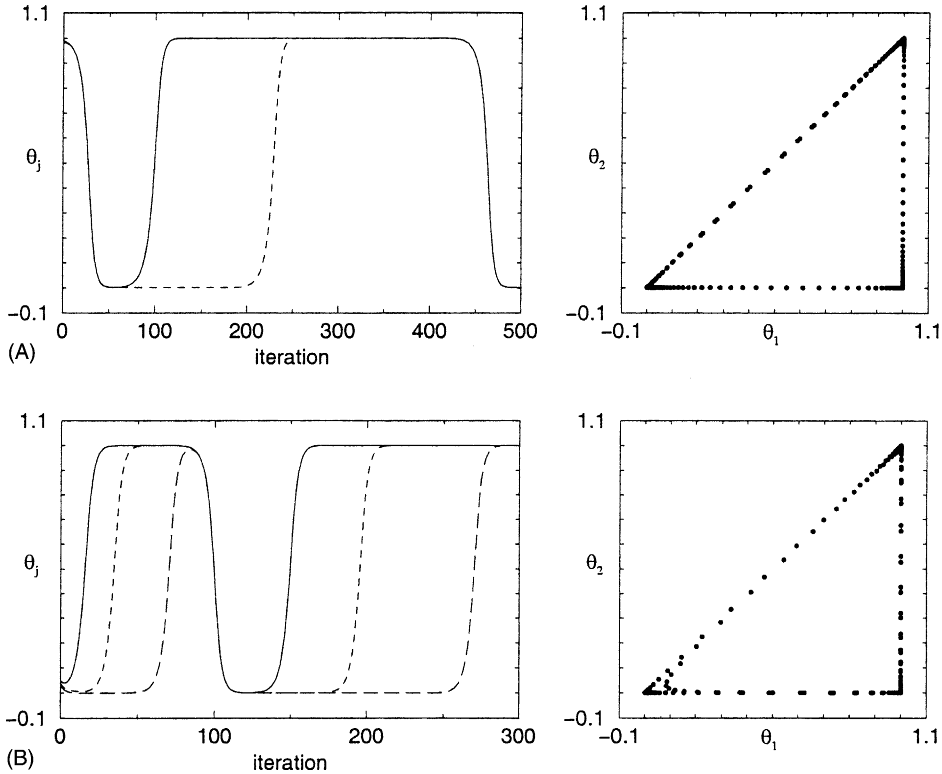

Fig. 5. (A) The evolution of the phases for three all-to-all coupled PRCs (left) and the projection into the θ_2–θ_3 phase-plane. (B) Same as (A) for four all-to-all PRCs.

A similar bound can be found for $N = 4$ oscillators: $a < a^* \approx 0.839$ then synchrony is unstable for four oscillators. We illustrate this point for $N = 3, 4$ oscillators in Fig. 5 . This shows the behavior of the map for $a = 0.2$ with initial data close to synchrony. The relative phases move around with longer and longer periods tending to synchrony for many iterates only to escape and drift around. This is quite similar to the approach of a dynamical system to a heteroclinic cycle. If we increase a past the critical value, then small perturbations from synchrony remain small and rapidly converge to the synchronous solution.

4. One-dimensional geometries

We now turn to one-dimensional geometries. The first case to consider is a chain of N coupled maps with nearest neighbor coupling:

$$\frac{\mathrm{d}\theta_j}{\mathrm{d}t} = 1 + \Delta(\theta_j)[\delta(\theta_{j-1}) + \delta(\theta_{j+1})] \tag{13}$$

with the stipulation that the end oscillators receive only one input for the linear chain or, in the case of a ring, $N + 1$ is identified with 1 and N with 0. Clearly one solution to this equation is the synchronous solution since $\Delta(0) = 0$. (Note that for the integrate-and-fire PRC, $\Delta(0) \neq 0$ so that a simple linear chain cannot synchronize. Indeed, the oscillators in the middle advance by an amount $2\Delta(0)$, while the ends only advance by an amount $\Delta(0)$ so synchronization is impossible.) One can ask if synchrony is stable and furthermore if there are other possible solutions.

The issue of stability remains open. In the case of a ring with $N = 3$, the network is actually all-to-all coupled and thus covered by our previous results. However, $N > 3$ remains an open problem. We conjecture that if the PRC is continuously differentiable at the origin, and if $0 < F'(0) < 1$, synchrony in both a ring and a linear chain is stable. This is certainly true for weak coupling since $F'(0) < 1$ implies that $\Delta'(0) < 0$ and thus the synchronous phase-locked state is stable (cf. Section 2.4). Furthermore, this is also consistent with the results for smooth-pulse coupling (Section 2.5).

4.1. *Waves in a ring*

In addition to synchrony, there are other possible solutions in a ring. The simplest such solution is a wave in which the timing interval between the firing of successive oscillators is constant. We now establish conditions for the existence of such a fixed timing wave by deriving an $(N-1)$-dimensional map valid near such a wave. As with the all-to-all coupled case, that map will advance the oscillator index as well as the phase. Suppose that oscillator N has fired and all the remaining oscillators coupled to N (e.g. $N-1$ and 1) have also been reset. The next oscillator to fire will be oscillator 1 since the sequence is assumed to be $1 \to 2 \to \cdots \to N$. The amount of time that it takes for oscillator 1 to reach firing is $1-\theta_1$ so that oscillator $j < N$ will have advanced to $\theta_j + 1 - \theta_1$ and oscillator N will have advanced to $1-\theta_1$. Oscillator 2 and oscillator N receive inputs from oscillator 1 (since it is nearest neighbor coupling) thus they both will receive a resetting pulse so that their respective phases are $F(1-\theta_1+\theta_2)$ and $F(1-\theta_1)$. We are now back to where we started but shifted forward one step. Thus, we obtain the following $(N-1)$-dimensional map:

$$\begin{aligned}
\theta_1' &= F(1-\theta_1+\theta_2) \\
\theta_2' &= 1-\theta_1+\theta_3 \\
\vdots &= \vdots \\
\theta_{N-2}' &= 1-\theta_1+\theta_{N-1} \\
\theta_{N-1} &= F(1-\theta_1).
\end{aligned}$$

This map gets iterated N times per wave but the map is the same at each step so that we need only consider one step for issues such as the existence of a non-trivial fixed point or the stability. We suppose that the time between successive firings is τ. Thus, we must have $1-\theta_1 = \tau$. We can use this to find the fixed points:

$$\begin{aligned}
\theta_{N-1} &= F(\tau) \\
\theta_{N-2} &= \tau + F(\tau) \\
\theta_{N-3} &= 2\tau + F(\tau) \\
\vdots &= \vdots \\
\theta_2 &= (N-3)\tau + F(\tau) \\
1-\tau &= F((N-2)\tau + F(\tau)).
\end{aligned}$$

From this, we see that there will be such a fixed point for the map if and only if

$$G(\tau, N) = F(F(\tau) + (N-2)\tau) + \tau = 1.$$

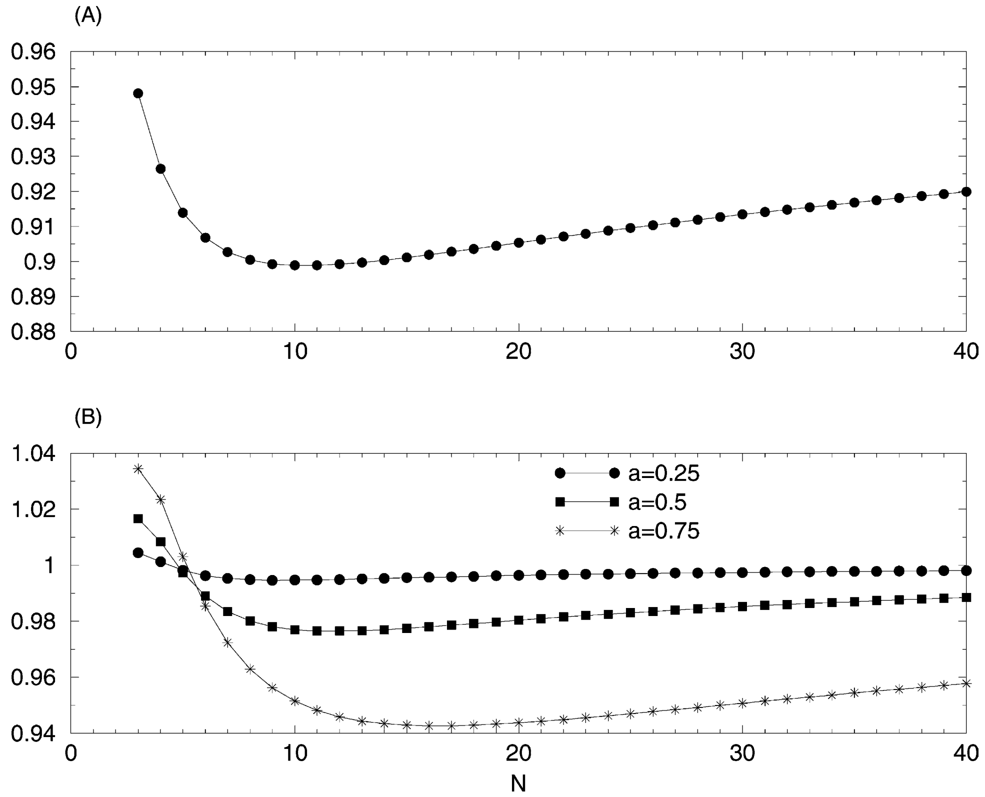

Fig. 6. The period as a function of the number of oscillators in the ring for: (A) the cortical neuron PRC; (B) the sine model at different amplitudes of coupling.

Suppose for the moment that the PRC is small so that $F(x) = x + \epsilon\Delta(x)$, where ϵ is small and positive. Then, upon expanding in ϵ to order 2 we find

$$\tau = \frac{1}{N} - \frac{\epsilon}{N}\left[\Delta\left(\frac{1}{N}\right) + \Delta\left(1-\frac{1}{N}\right)\right] + \frac{\epsilon^2}{N^2}\left[\left(\Delta\left(\frac{1}{N}\right) + \Delta\left(1-\frac{1}{N}\right)\right)\left(\Delta'\left(\frac{1}{N}\right) - \Delta\left(1-\frac{1}{N}\right)\right) + N\Delta\left(1-\frac{1}{N}\right)\Delta'\left(1-\frac{1}{N}\right)\right].$$

Thus, the timing difference is roughly the length of an uncoupled cycle divided by the number of oscillators. If the PRC is anti-symmetric as is the case for the radial isochron clock, then the firing interval is $1/N + \mathrm{O}(\epsilon^2)$. Since it is a simple matter to numerically solve $G(\tau, N) = 1$ we do so in Fig. 6 for the model (3) which fits Reyes data and for the standard sine model $\Delta(x) = -a\sin(2\pi x)/(2\pi)$ for a variety of values of a. Rather than plot τ, we instead plot $T = N\tau$ which is the period of a wave. Thus the figures represent a “dispersion” curve for the ring of coupled PRCs. We point out that the neurally motivated PRC (top panel) has a period that is always less than the uncoupled period. This is a consequence of the fact that Δ is non-negative and the effect of a pulse is to always advance the phase. In contrast, the sine model can both advance and delay the phase and this is shown by the fact that the period is slightly longer for small values of N.

Local stability is determined by linearizing about the fixed point. The resulting matrix has the form

$$B_N = \begin{pmatrix} -\alpha_N & \alpha_N & 0 & 0 & \cdots & 0 \\ -1 & 0 & 1 & 0 & \cdots & 0 \\ \vdots & \vdots & \vdots & \vdots & \vdots & \vdots \\ -1 & 0 & \cdots & 0 & 0 & 1 \\ -\alpha_1 & 0 & 0 & 0 & \cdots & 0 \end{pmatrix},$$

where $\alpha_N = F'((N-2)\tau + F(\tau))$ and $\alpha_1 = F'(\tau)$. A direct calculation shows that the characteristic polynomial of B_N is just

$$P(\lambda) = \lambda^N + \alpha_N(\lambda^{N-1} + \cdots + \lambda) + \alpha_N\alpha_1.$$

The "Jury" test [7] is a test similar to the Routh–Hurwitz test which allows us to determine when the roots of P lie inside the unit circle. First we note that α_N, α_1 are both positive by the monotonicity of F. Applying this test to $P(\lambda)$ shows that the roots lie in the unit circle if and only if: (i) $\alpha_N < 1$; (ii) $\alpha_1\alpha_N < 1$; (iii) $1 + \alpha_N\alpha_1 > \alpha_N$. The last condition is trivially satisfied if the first two are satisfied. These conditions are quite intuitively satisfying and very simple to verify. Condition (ii) says that the slope of the PRC must be negative as ϕ approaches 1. This condition is always met in the cortical models when the coupling is excitatory. The second condition is similar to our condition for stability of synchrony for the two neuron network.

We cannot use the map to look at the stability of synchrony since the map is defined under the strict firing order assumption. Small perturbations of the wave maintain this ordering. However, the ordering will not be maintained for the synchronous solution.

Numerical solutions indicate that the waves for $N \leq 10$ are unstable for the model (3). For the sine model, (2), the stability depends on a; for a small enough we expect that all waves with $N > 4$ will be stable. This is because when $a \ll 1$ the weakly coupled PRCs become the simple phase models:

$$\frac{d\phi_j}{dt} = \Delta(\phi_j - \phi_{j+1}) + \Delta(\phi_j - \phi_{j-1}).$$

The phase differences between the successive oscillators are $1/N$ and it follows from Ermentrout [8] that a sufficient condition for stability is that $\Delta'(1/N) < 0$. For the sine model this means that $\cos(2\pi/N) > 0$ so that $N > 4$. However, for larger values of a bigger rings are required to get a stable pattern.

This result generalizes the result of Canavier et al. and Dror et al. to bi-directional coupling and to arbitrary rings of oscillators. However, the results here are local stability results whereas the results from the Canavier group are global.

4.2. Chains of PRCs

If we eliminate the coupling between the 1st and the Nth oscillator in the ring, we are left with a one-dimensional chain of oscillators. If the coupling is bi-directional and symmetric, then one possible solution is synchrony. It is difficult to create a map for this case due to the fact that there is no reason to believe that ordering will be maintained as was the case for global coupling. Thus, stability of this state is difficult to prove in general. Even the case of a three oscillator chain is difficult due to the many possible cases and firing orders. If the PRC is small enough then we can appeal to results for a weakly coupled chain (Section 2.4) which imply that synchrony is stable if $\Delta'(0) < 0$. However, if the PRC is not continuously differentiable at the origin, as seems to be the

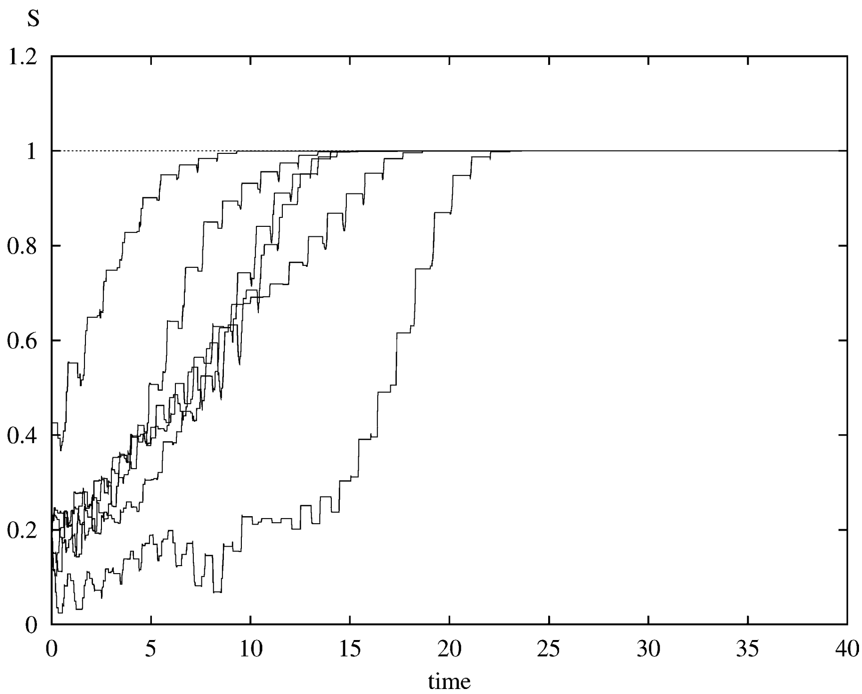

Fig. 7. Synchronization in a chain of 20 oscillators starting at random phases and using the PRC from Fig. 3. $S = 1$ is the perfectly synchronized state.

case for cortical neurons, then even this rather restrictive result cannot be applied. Instead, we must resort to numerical simulations. Fig. 7 shows the results of a simulation of a chain of 20 nearest neighbor coupled oscillators using the PRC from Eq. (3) with $a = 1.116, b = 0.775$, and $c = 10.2$ which matches the cortical PRC shown in Fig. 3. We plot a synchrony index for five different initial conditions in which the phases are either randomly distributed over [0, 1] or biased toward a traveling wave solution. The synchrony index, S is defined as

$$S = \sqrt{A^2 + B^2}, \quad A = \frac{1}{20} \sum_{j=1}^{N} \sin 2\pi\theta_j, \quad B = \frac{1}{20} \sum_{j=1}^{N} \cos 2\pi\theta_j.$$

If the phases, θ_j are uniformly dispersed around the circle, then $S = 0$ and if they are perfectly synchronized, $S = 1$. Kuramoto [19, p. 71] defines a similar index of synchrony for a globally coupled array of weakly coupled oscillators. For *rings*, the random initial data generally converge to a synchronous solution. However, the biased initial data converge to a traveling wave which has a small synchrony index as the phases are nearly evenly dispersed. We conjecture that if synchrony is stable for pairwise interactions, then it will be stable for chains of nearest neighbor connectivity as long as the coupling is not too strong. This is completely consistent with the results of smooth pulse coupling in Section 2.5. We remark that the behavior of coupled chains is different from the behavior of chains of phase-difference models such as those analyzed by Kopell and Ermentrout [18]. In generic phase-difference models, synchrony is not even a solution unless one makes adjustments at the ends. Such adjustments are unnecessary with PRCs since there is no effect from an input coming at the exact moment a cell fires ($\Delta(0) = \Delta(1) = 0$).

5. Two-dimensional arrays of coupled oscillatory neurons

We consider a network of neural oscillators that are arranged in an $N \times N$ square array. Each oscillator is bi-directionally coupled to its nearest neighbors through a PRC. In this section, we show that for the sine PRC persistent *circular waves* can be set up in certain size arrays. That is, the firings proceed systematically in a circular fashion on the array.

5.1. A simulation of the wave

We first simulate the wave, to determine the times that the various neurons fire relative to the neuron in the top leftmost corner. That is, the time of firing of the θ_{00} is chosen to be the reference zero time in each period that the wave goes around. The algorithm is as follows. Each neuron is represented as a variable in a two-dimensional array. The time this neuron last fired is stored in this variable. Thus, *as the wave passes through the array*, each cell reflects either the firing time (with respect to θ_{00}) from the previous cycle of the wave passing through it, or if the wave has struck it in this cycle, the (current) time it fired. The variables are updated to their most recent value of the firing time, after θ_{00}. We start of the simulation with a certain guess at the firing times of the neuron (detailed below), and see if, as one wave after the other passes through, the system settles into an invariant firing sequence. The wave passing through is implemented by first allowing the θ_{00} neuron to fire, then searching the array for that neuron θ_{ij} that is closest to firing. All the neurons are updated to reflect their phases just before θ_{ij} fires. Finally, the phase of this θ_{ij} is reset to 0, and simultaneously the phases of its (four) nearest neighbors are affected by the PRC. This is repeated until θ_{00} fires again. This leads to a sequence that presumably persists and corresponds to a stable rotating wave.

The initial firing times that we choose for the simulation can be described as follows. The array can be visualized as being roughly composed of consecutive *rings* (in analogy with the term *circular* wave). Then, if we consider successive rings, we notice that firings must proceed (counter)clockwise on each ring. To guess at the firing times of the neurons on a ring, we choose the following. Consider the outermost ring of $4(N-1)$ neurons. Since the θ_{00} neuron fires at the time $t = 0$, and again at (roughly) $t = 1$, the other neurons are setup to fire $\alpha = 1/4(N-1)$ apart, going round on the ring. We can then choose, for a clockwise wave, the firing times for neurons on the outer ring to be α for θ_{01}, 2α for θ_{02}, and so on. The next inner ring is initialized similarly, with θ_{11} set to 0, and the other neurons $\beta = 1/4(N-3)$ apart going clockwise around. We continue in this manner until all the neurons have been initialized.

5.2. The exact system of equations

We now consider the algebraic conditions necessary for a rotating wave with the sinusoidal PRC. There are N^2 unknowns that need to be determined for an $N \times N$ array: the period of the oscillation and the $N^2 - 1$ times relative to the upper left corner. From reflection symmetry only a quarter of these actually need to be found. This leads to $(\frac{1}{2}N)^2$ unknowns. We derive the equations for phase-locking for the 4×4 array and then find the roots of this. We compare them to the simulated times.

5.3. The 4×4 *array*

The simplest case to study circular waves in square arrays is $N = 4$.

5.3.1. Results of the simulation

We considered a PRC $\Delta(\phi) = -a\sin(2\pi\phi)/(2\pi)$ with a value of $a = 0.2$. The following table contains the steady state firing times of the different neurons. (Note that the actual simulations were done on the interval

$0 < \phi < 2\pi$ for convenience; here we scale the times back to the interval $0 < \phi < 1$.)

$0.0/(2\pi)$	$0.337/(2\pi)$	$1.172/(2\pi)$	$1.564/(2\pi)$
$5.864/(2\pi)$	$0.018/(2\pi)$	$1.158/(2\pi)$	$1.901/(2\pi)$
$5.029/(2\pi)$	$4.710/(2\pi)$	$3.146/(2\pi)$	$2.736/(2\pi)$
$4.692/(2\pi)$	$4.300/(2\pi)$	$3.465/(2\pi)$	$3.128/(2\pi)$

$\tau = 6.256/(2\pi) \approx 0.9956$ is the period of the wave, i.e. the time that θ_{00} fires again. Note that the period is shorter than the uncoupled period of 1 but only by a very small amount.

A pattern of firing times can be discerned by perusing the table of values from the simulation. The following table summarizes the various firing times in terms of four $((\frac{1}{2}N)^2)$ unknowns:

0	α	$\tau/4 - \beta$	$\tau/4$
$\tau - \beta$	γ	$\tau/4 + \gamma$	$\tau/4 + \alpha$
$3\tau/4 + \alpha$	$3\tau/4 + \gamma$	$\tau/2 + \gamma$	$\tau/2 - \beta$
$3\tau/4$	$3\tau/4 - \beta$	$\tau/2 + \alpha$	$\tau/2$

The structure of this table depends crucially on the fact that the PRC we use is odd-symmetric. Like the work of Paullet and Ermentrout [21], we exploit this symmetry to reduce the number of equations. If $\Delta(-\phi) \neq -\Delta(\phi)$ then there can generally be no such simplification. However, the simulation scheme works for any PRC, Δ such that $|\Delta'(\phi)| < 1$ (i.e. $F(\phi)$ is invertible).

From this table, we can derive a set of four equations. Consider the θ_{00} neuron. When it fires at time $t = 0$, its phase is 0 at that instant. The phase then continues to increase, until one of its neighbors fires. Based on the simulations we expect that going around in a wave the neuron θ_{01} (rather than θ_{10}) will fire first. At this point the phase of θ_{00} changes from α to $F(\alpha)$. Once more, the phase of θ_{00} continues to grow independently till a time $\tau - \beta$, when θ_{10} fires, and disturbs its phase to $F(F(\alpha) + (\tau - \beta - \alpha))$. With no other firings to affect it, it can continue to rise until 1, when it fires and must be reset to 0. Thus the following equation must hold:

$$F(F(\alpha) + (\tau - \beta - \alpha)) + \beta = 1.$$

Similarly, we can write three other equations by choosing three other oscillators to get a complete system:

$$\begin{aligned} &F(F(\alpha) + (\tau - \beta - \alpha)) + \beta = 1, \qquad F(F(F(\beta) + \gamma) + 0.75\tau + \alpha - \gamma) + \beta = 1,\\ &F(F(F(0.25\tau - \beta - \alpha) + 0.75\tau + \beta) + \gamma) + \alpha - \gamma = 1,\\ &F(F(F(F(\alpha - \gamma) + 0.25\tau + \gamma - \alpha) + 0.5\tau) + 0.25\tau - \beta - \gamma) + \gamma + \beta = 1. \end{aligned} \tag{14}$$

(In Paullet and Ermentrout, $\tau = 1$, $\alpha = \beta$, and $\gamma = 0$ so that there was a single algebraic equation.)

The system of Eq. (14) can be solved for α, β, γ and τ, using Newton's method. Furthermore, we can use a continuation package such as XPPAUT to study how the roots evolve as the magnitude a increases.

5.4. *The* 6×6 *array*

The next case to study is $N = 6$. Again, we carry out a simulation, and compare the results to a computation from a system of exact equations. Proceeding as outlined above we obtain the following array of firing times:

$0.0/(2\pi)$	$0.125/(2\pi)$	$0.447/(2\pi)$	$0.960/(2\pi)$	$1.345/(2\pi)$	$1.563/(2\pi)$
$6.036/(2\pi)$	$6.162/(2\pi)$	$0.287/(2\pi)$	$1.046/(2\pi)$	$1.471/(2\pi)$	$1.688/(2\pi)$
$5.651/(2\pi)$	$5.737/(2\pi)$	$6.188/(2\pi)$	$1.497/(2\pi)$	$1.851/(2\pi)$	$2.011/(2\pi)$
$5.138/(2\pi)$	$4.978/(2\pi)$	$4.624/(2\pi)$	$3.061/(2\pi)$	$2.609/(2\pi)$	$2.523/(2\pi)$
$4.816/(2\pi)$	$4.598/(2\pi)$	$4.173/(2\pi)$	$3.414/(2\pi)$	$3.034/(2\pi)$	$2.909/(2\pi)$
$4.690/(2\pi)$	$4.473/(2\pi)$	$4.087/(2\pi)$	$3.575/(2\pi)$	$3.252/(2\pi)$	$3.127/(2\pi)$

As the above table shows, this is a wave circling on a six-dimensional array. The wave is stable and (locally) attracting. Fig. 8 shows a plot of these relative phases. The outermost ring of 20 oscillators looks like a traveling wave that covers one full cycle as the perimeter is traversed. Similarly the middle ring of 12 oscillators is also a traveling wave. The inner ring of four oscillators consists of cells one quarter of a cycle apart. Thus, these apparently stable patterns look like nested rings of coupled maps, nearly synchronized along the diagonals. We point out that the patterns here are the direct analogs of those found by Paullet and Ermentrout [21] in arrays of weakly coupled oscillators. The pattern of phases in two dimensions is like a pinwheel such as seen in the analysis of the Ginzberg–Landau equation [13,14,22]:

$$z_t = z(1 + \mathrm{i}\omega - z\bar{z}) + \nabla^2 z.$$

In Fig. 9, we show the period of the rotating wave as a function of the strength of the coupling, a for the four- and six-dimensional square arrays. We note that this is not monotonic.

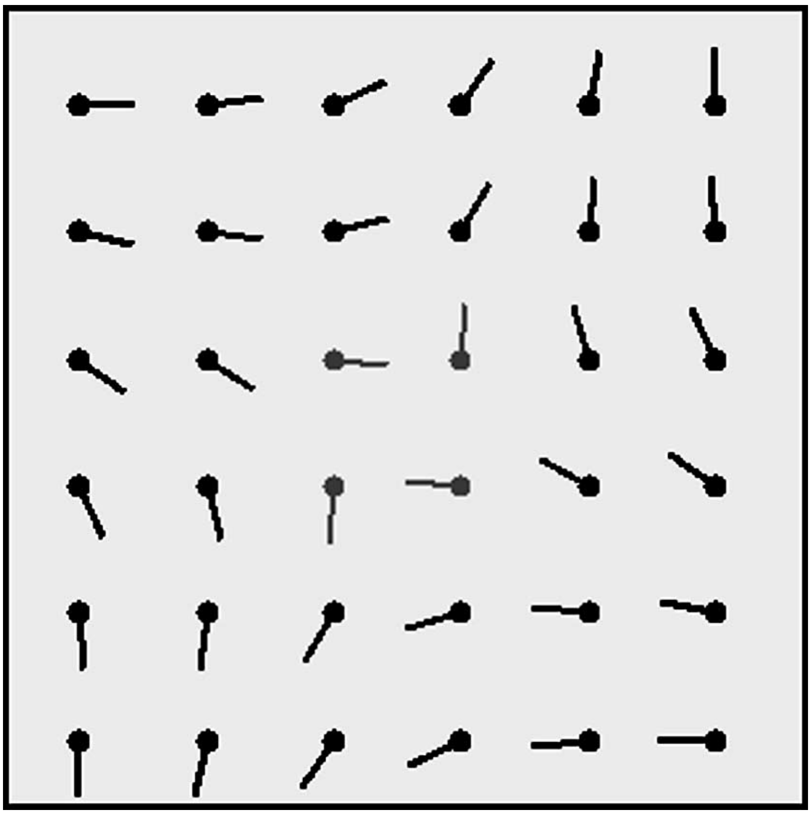

Fig. 8. The relative phases for the 6×6 array in the sine model. Lines denote the angle relative to the upper left corner. Outer, middle, and inner "rings" are different gray scales.

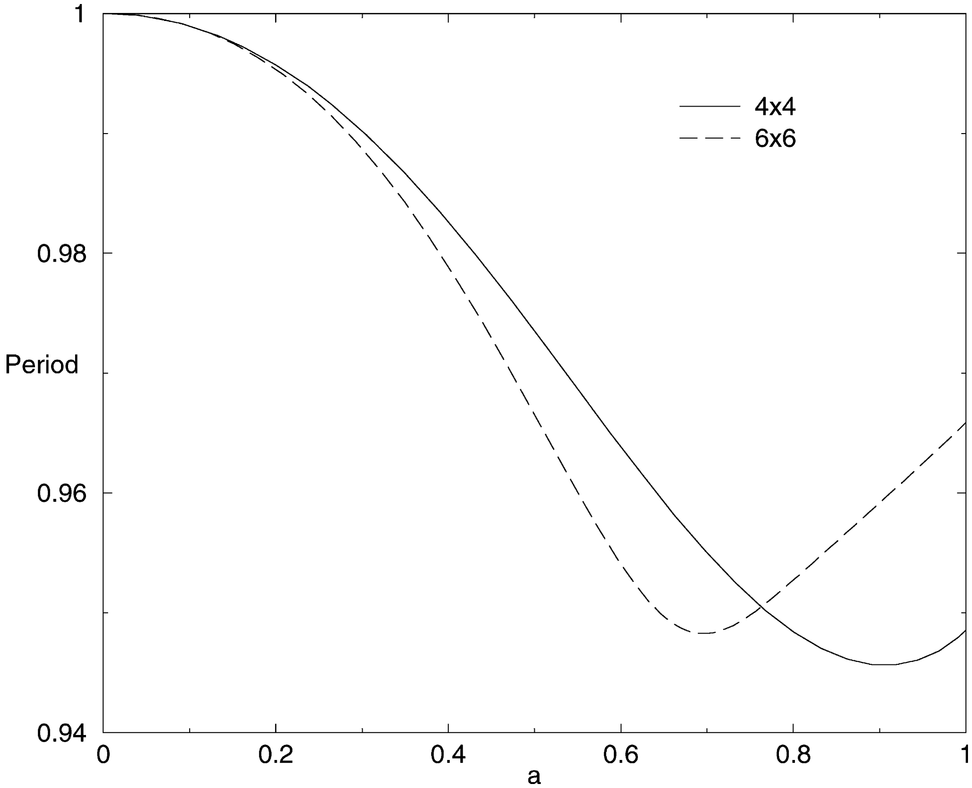

Fig. 9. The period as a function of the strength of coupling in a square array for the sine model.

5.5. Larger two-dimensional arrays

We have extended our simulations to arbitrary sized arrays. Simulations show similar waves. The analyses based on writing an analytical set of equations grows increasing difficult to implement, however. We note that the small arrays of odd-dimension (e.g. 5×5) seem to have only the synchronous solution (at least for the initial conditions implemented in above). However, preliminary results on large arrays show that the dependence on the evenness of the dimension is an artifact of small dimensionality. We expect these circular waves exist in all even N-dimensional ($N \geq 4$) arrays and sufficiently large odd-dimensioned arrays. A general existence is still an open question as is the rigorous determination of stability.

6. Discussion

We have generally examined a number of networks of coupled PRCs. Under certain assumptions (i.e. a fixed firing sequence) it is possible to reduce these to discrete maps. However, the existence of such a map depends on maintaining this fixed firing sequence. Thus, the issue of heterogeneity in uncoupled frequency becomes an important one for the all-to-all networks. For then, near synchrony, it is possible for the order of firing to be changed. On the other hand, with heterogeneity, we do not expect exactly synchronous solutions. Instead, we expect that the oscillators will fire in order of their uncoupled frequency. Small perturbations will not destroy this order so that our techniques are probably applicable. Heterogeneity in coupling is significantly more difficult.

The development of a theory for general all-to-all systems remains to be found. For the ring models where there is a fixed firing sequence bounded away from synchrony, small differences in the oscillators will not affect the map as the sequence will be maintained. The maps for linear chains and the two-dimensional systems remain to be described. We note that it is probably possible (albeit tedious) to prove the synchrony of the rotating waves in the two-dimensional lattices. The idea is to exploit the fact that there is a fixed firing sequence. This allows us to define a local linearization of the map and from this determine whether synchrony is stable. All numerical simulations seem to point to stability at least for the simple sinusoidal PRC. Ideally, a general theorem analogous to that in [8] could be proven.

Canavier et al. and Dror et al. have concentrated their efforts on computing and analyzing the PRCs for coupled "burst-like" neurons. This is in some ways a much more difficult problem than that which we have derived here. In bursting neurons the effect of one oscillator on the other can be prolonged. Furthermore, the length of time of the effect can depend on the inputs to that oscillator. Effects of such a large perturbation can affect the next cycle as well. Thus, the maps that one derives from coupled bursters are much more challenging to analyze. In the present paper, the interactions are presumed to be very short-lasting compared to the period of the oscillators. For example, cortical excitatory synapses typically last only 2–5 ms while the period of oscillations varies from 25 to 100 ms. This allows us to ignore the possibility of inputs "bleeding" over into the next cycle.

Acknowledgements

We benefited from Jon Rubin's useful comments on the manuscript. This work was partially supported by the NSF grants DMS-9972913 and NIMH.

Appendix A

Proof of theorem. We define the following N diagonal matrices, d_k, $k = 1, \dots, (N-1)$, as follows: d_0 is the $(N-1)$-dimensional diagonal matrix with all its (non-zero) elements α_0's, d_1 with α_1's, and the other d_i's having both α_0's and α_1's. $d_2 = \mathcal{D}(\alpha_1, \alpha_1, \dots, \alpha_1, \alpha_0)$, $d_3 = \mathcal{D}(\alpha_1, \alpha_1, \dots, \alpha_0, \alpha_0)$, and so on with d_i having as its last $(i-1)$ elements α_0 (and the others α_1), where $\mathcal{D}$ stands for the $(N-1) \times (N-1)$ diagonal matrix. Also, let

$$E = \begin{bmatrix} -1 & 1 & 0 & 0 & \cdots \\ -1 & 0 & 1 & 0 & \cdots \\ -1 & 0 & 0 & 1 & \\ \vdots & & & & \ddots \\ -1 & 0 & & & 0 \end{bmatrix}.$$

If $B = ED_{n-1}, \dots, ED_1ED_0$, then the eigenvalues of B are of the form $\alpha_0^p \alpha_1^{N-p}$ with $1 \le p \le N-1$.

Proof. Let us consider the product B above. We claim that the following matrix S is a similarity transformation that diagonalizes B with the required eigenvalues on the diagonal. S is the $(N-1) \times (N-1)$ matrix with all elements on the diagonal, and above it, unity, and zero otherwise. That is,

$$S=\begin{bmatrix} 1 & & \cdots & & 1\\ 0 & 1 & & & \\ \vdots & \ddots & \ddots & & \vdots\\ \vdots & & \ddots & 1 & \\ 0 & \cdots & \cdots & 0 & 1 \end{bmatrix}$$

with an inverse

$$S^{-1}=\begin{bmatrix} 1 & -1 & 0 & \cdots & 0\\ 0 & 1 & \ddots & \ddots & \vdots\\ \vdots & \ddots & \ddots & \ddots & 0\\ \vdots & & \ddots & 1 & -1\\ 0 & \cdots & \cdots & 0 & 1 \end{bmatrix}.$$

Thus we need to show that $S^{-1}BS$ is a diagonal matrix. We proceed as follows: it is a simple matter to evaluate the product ED_1ED_0S which is of the following general form:

$$ED_1ED_0S=\begin{bmatrix} 0 & -\alpha_0\alpha_1 & 0 & \cdots & 0\\ & & \ddots & \ddots & \vdots\\ \vdots & \vdots & & \ddots & 0\\ 0 & -\alpha_0\alpha_1 & \cdots & & -\alpha_0\alpha_1\\ \alpha_0\alpha_1 & 0 & \cdots & & 0 \end{bmatrix}.$$

Next, we make the following claim: every matrix product up to the kth factor $ED_k,\ldots,ED_1ED_0S$ is of the general form

$$P_k=ED_k,\ldots,ED_1ED_0S=\begin{bmatrix} 0 & & \cdots & & 0 & -\alpha_0\alpha_1^k & 0 & \cdots & 0\\ \vdots & & & & \vdots & & \ddots & \ddots & \vdots\\ & & & & & \vdots & & \ddots & 0\\ 0 & & \cdots & & 0 & -\alpha_0\alpha_1^k & \cdots & & -\alpha_0\alpha_1^k\\ \alpha_0^k\alpha_1 & \alpha_0^{k-1}\alpha_1^2 & \cdots & \alpha_0^2\alpha_1^{k-1} & \alpha_0\alpha_1^k & 0 & \cdots & \cdots & 0\\ 0 & \alpha_0^{k-1}\alpha_1^2 & & \vdots & \vdots & \vdots & & & \vdots\\ & \ddots & & & & & & & \\ \vdots & & \ddots & \alpha_0^2\alpha_1^{k-1} & \vdots & \vdots & & & \vdots\\ 0 & \cdots & & 0 & \alpha_0\alpha_1^k & 0 & \cdots & \cdots & 0 \end{bmatrix}.$$

We remark the following characteristics of this matrix: the $(N-1)$-dimensional matrix above is made up of two submatrices of dimensions k and l with $l=(N-1)-k$. Let us call the 'lower triangular' submatrix occupying the upper right $l\times l$ corner of P_k, the $\mathcal{L}$ (sub)matrix, and the 'upper triangular' submatrix occupying the bottom left $k\times k$ corner of P_k, the $\mathcal{K}$ (sub)matrix. (We note all other elements of P_k are identically zero.) All elements of $\mathcal{L}$ are identical, and equal to $-\alpha_0\alpha_1^k$. All elements in the ith column of $\mathcal{K}$ are identical, and equal to $\alpha_0^{k+1-i}\alpha_1^i$. We next consider the product of P_k with the next (premultiplying) factor $P_{k+1}=ED_{k+1}P_k$ in $S^{-1}BS$. If our original claim is to be true, the matrix P_{k+1} must be of the same general form that we described for P_k. Except that for P_{k+1}, its $\mathcal{K}$ matrix is of dimension $(k+1)$ (and $\mathcal{L}$ is one dimension smaller). We verify this is indeed the case. We note that D_{k+1} is a diagonal matrix with the last $k+1$ elements α_0 (the first $N-1-k$ elements α_1). Hence, we observe that the product $D_{k+1}P_k$ is simply obtained by multiplying the elements of $\mathcal{L}$ in P_k by α_1, and those of $\mathcal{K}$ by α_0! We also notice that under (pre)multiplication by E, every jth column $(r_1,r_2,\dots,r_{N-2},r_{N-1})^{\mathrm{T}}$ in the multiplicand matrix is simply permuted to $(-r_1+r_2,-r_{1+}r_3,\dots,-r_1+r_{N-2},-r_1)^{\mathrm{T}}$. The product $ED_{k+1}P_k$ is then of the desired form. Proceeding to write $BS\equiv P_{N-1}$ we obtain the upper triangular matrix:

$$BS=\begin{bmatrix} \alpha_0^{N-1}\alpha_1 & \alpha_0^{N-2}\alpha_1^2 & \cdots & \alpha_0^2\alpha_1^{N-2} & \alpha_0\alpha_1^{N-1} \\ 0 & \alpha_0^{N-2}\alpha_1^2 & & \vdots & \vdots \\ \vdots & & \ddots & & \\ & & \ddots & \alpha_0^2\alpha_1^{N-2} & \vdots \\ 0 & & \cdots & 0 & \alpha_0\alpha_1^{N-1} \end{bmatrix}.$$

It can easily be verified that premultiplying by S^{-1} (given above) then sets all the elements besides those on the diagonal to zero. Hence the eigenvalues of B follow as proposed. □

References

[1] J.T. Ariaratnam, S.H. Strogatz, Phase diagram for the Winfree model of coupled nonlinear oscillators, Phys. Rev. Lett. 86 (2001) 4278–4281.
[2] P.C. Bressloff, S. Coombes, Symmetry and phase-locking in a ring of pulse-coupled oscillators with distributed delays, Physica D 126 (1999) 99–122.
[3] P.C. Bressloff, S. Coombes, Dynamics of strongly coupled spiking neurons, Neural Comput. 12 (2000) 91–129.
[4] J. Buck, Synchronous rhythmic flashing in fireflies, II, Quart. Rev. Biol. 63 (1988) 265–289.
[5] C.C. Canavier, D.A. Baxter, J.W. Clark, J.H. Byrne, Control of multistability in ring circuits of oscillators, Biol. Cyber. 80 (1999) 87–102.
[6] R. Dror, C.C. Canavier, R.J. Butera, J.W. Clark, J.H. Byrne, A mathematical criterion based on PRCs for stability in a ring of coupled oscillators, Biol. Cyber. 80 (1999) 11–23.
[7] L. Edelstein-Keshet, Mathematical Models in Biology, McGraw-Hill, New York, 1988, pp. 58–59.
[8] G.B. Ermentrout, Stable periodic solutions to discrete and continuum arrays of weakly coupled nonlinear oscillators, SIAM J. Appl. Math. 52 (1992) 1665–1687.
[9] B. Ermentrout, Type I membranes, phase resetting curves, and synchrony, Neural Comput. 8 (1996) 979–1001.
[10] G.B. Ermentrout, N. Kopell, Multiple pulse interactions and averaging in systems of coupled neural oscillators, J. Math. Biol. 29 (1991) 195–217.
[11] L. Glass, M. Mackey, From Clocks to Chaos. The Rhythms of Life, Princeton University Press, Princeton, NJ, 1988.
[12] C.M. Gray, Synchronous oscillations in neuronal systems: mechanisms and functions, J. Comput. Neurosci. 1 (1994) 11–38.
[13] J.M. Greenberg, Spiral waves for λ–ω systems, SIAM J. Appl. Math. 39 (1982) 301–309.
[14] P.S. Hagan, Spiral waves in reaction–diffusion systems, SIAM J. Appl. Math. 42 (1982) 762–786.
[15] D. Hansel, G. Mato, C. Meunier, Synchrony in excitatory neural networks, Neural Comput. 7 (1995) 307–337.
[16] F.C. Hoppensteadt, E.M. Izhikevich, Weakly Connected Neural Networks, Springer, New York, 1997.
[17] N. Kopell, Towards a theory of modeling central pattern generators, in: A.H. Cohen, S. Rossignol, S. Grillner (Eds.), Neural Control of Rhythms, Wiley, New York, 1988.

[18] N. Kopell, B. Ermentrout, Symmetry and phase-locking in chains of weakly coupled oscillators, Commun. Pure Appl. Math. 39 (1986) 623–660.
[19] Y. Kuramoto, Chemical Oscillations, Waves, and Turbulence, Springer, Berlin, 1984.
[20] R.M. Mirollo, S.H. Strogatz, Synchronization of pulse-coupled biological oscillators, SIAM J. Appl. Math. 50 (1990) 1645–1662.
[21] J. Paullet, G.B. Ermentrout, Stable rotating waves in two-dimensional discrete active media, SIAM J. Appl. Math. 54 (1994) 1720–1744.
[22] J. Paullet, G.B. Ermentrout, W.C. Troy, The existence of spiral waves in an oscillatory reaction–diffusion system, SIAM J. Appl. Math. 54 (1994) 1386–1401.
[23] A.D. Reyes, E.E. Fetz, Two modes of interspike interval shortening by brief transient depolarizations in cat neocortical neurons, J. Neurophysiol. 69 (1993) 1661–1672.
[24] A.D. Reyes, E.E. Fetz, Effects of transient depolarizing potentials on the firing rate of cat neocortical neurons, J. Neurophysiol. 69 (1993) 1673–1683.
[25] R. Stoop, K. Schindler, L.A. Bunimovich, Neocortical networks of pyramidal neurons: from local locking and chaos to macroscopic chaos and synchronization, Nonlinearity 13 (2000) 1515–1529.
[26] R. Stoop, L.A. Bunimovich, W.-H. Steeb, Generic origins of irregular spiking in neocortical networks, Biol. Cyber. 83 (2000) 481–489.
[27] C. van Vreeswijk, L.F. Abbott, G.B. Ermentrout, When inhibition, not excitation synchronizes neural firing, J. Comput. Neurol. 1 (1994) 313–321.
[28] A.T. Winfree, Biological rhythms and the behavior of populations of coupled oscillators, J. Theoret. Biol. 16 (1967) 15–42.
[29] A.T. Winfree, The Geometry of Biological Time, Springer, New York, 1980.